European Radiology
https://doi.org/10.1007/s00330-018-5643-4

BREAST

Diagnostic performance of initial enhancement analysis using ultra-fast dynamic contrast-enhanced MRI for breast lesions

Mariko Goto[1] · Koji Sakai[1] · Hajime Yokota[2] · Maki Kiba[3] · Mariko Yoshida[1] · Hiroshi Imai[4] · Elisabeth Weiland[5] · Isao Yokota[6] · Kei Yamada[1]

Received: 10 January 2018 / Revised: 14 June 2018 / Accepted: 29 June 2018

Abstract

Objectives To assess the diagnostic value and contribution to BI-RADS categorisation of initial enhancement on ultra-fast DCE-MRI for differentiating malignant and benign breast lesions.

Methods The institutional review board approved this study, and written informed consent was obtained from each participant. Both ultra-fast DCE-MRI for initial enhancement analysis and conventional MRI were performed on 200 subjects with a total of 215 lesions (147 malignant and 68 benign). BI-RADS categorisation of enhancing lesions was performed using the conventional MRI. Two initial enhancement measures, time to enhancement (TTE) and maximum slope (MS), were derived from the ultra-fast DCE-MRI. Diagnostic performance and the additional diagnostic value of adding TTE and MS to BI-RADS were evaluated.

Results Both TTE and MS showed significant differences between malignant and benign breast lesions in masses (TTE, p <.001; MS, p = .006) and non-mass enhancement (NME) (TTE, p <.001; MS, p <.001). For masses, the AUC of TTE+MS combined with BI-RADS (0.864) was better than BI-RADS alone (0.823, p = .065). For NME, the AUC of TTE+MS combined with BI-RADS (0.923) was significantly larger than BI-RADS alone (0.865, p = .036), and diagnostic specificity improved by 40.9% (p = .005), without a significant decrease in the sensitivity (p = .083).

Conclusion Initial enhancement analysis using ultra-fast DCE-MRI is especially useful for increasing the diagnostic performance of NME in breast MRI.

Key Points

- *Ultra-fast dynamic MRI effectively differentiates benign from malignant breast lesions.*
- *Ultra-fast dynamic MRI contributes to BI-RADS categorisation in non-mass enhancement.*
- *Management of non-mass breast lesions becomes more appropriate.*

Keywords Breast neoplasms · Magnetic resonance imaging · Contrast media · Kinetics · Classification

✉ Mariko Goto
gomari@koto.kpu-m.ac.jp

[1] Department of Radiology, Graduate School of Medical Science, Kyoto Prefectural University of Medicine, 465 Kajiicho, Kawaramachi Hirokoji, Kamigyoku, Kyoto 602-8566, Japan

[2] Department of Radiology, Chiba University Hospital, Chiba, Japan

[3] Department of Radiology, Japanese Red Cross Kyoto Daini Hospital, Kyoto, Japan

[4] Siemens Healthcare K.K., Tokyo, Japan

[5] Siemens Healthcare GmbH, Erlangen, Germany

[6] Department of Biostatistics, Graduate School of Medical Science, Kyoto Prefectural University of Medicine, Kyoto, Japan

Abbreviations

ACR	American College of Radiology
BI-RADS	Breast imaging reporting and data system
CI	Confidence interval
DCIS	Ductal carcinoma in situ
FOV	Field of view
GRAPPA	Generalised autocalibrating partial parallel acquisition
HER2	Human epidermal growth factor receptor type 2
HR	Hormone receptor
IDC	Invasive ductal carcinoma
ILC	Invasive lobular carcinoma
IQR	Interquartile range
MS	Maximum slope

Published online: 07 August 2018

NME	Non-mass enhancement
TTE	Time to enhancement
T2WI	T2-weighted imaging
TWIST	Time-resolved angiography with interleaved stochastic trajectories
VIBE	Volume-interpolated breath-hold examination

Introduction

Dynamic contrast-enhanced (DCE) magnetic resonance imaging (MRI) is now well established in clinical practice as having high sensitivity for the detection of breast cancer. The American College of Radiology (ACR) Breast Imaging Reporting and Data System (BI-RADS) MRI lexicon [1] is the most widely used guide for describing and categorising enhancing breast lesions on DCE-MRI.

In the BI-RADS MRI lexicon, the morphology of enhancing breast lesions is given priority over their kinetic features. For differentiating benign from malignant breast lesions on MRI, the effectiveness of initial enhancement analysis using high-temporal resolution images has been reported [2–5]. However, spatial resolution has to be sacrificed in this ultrafast imaging, and this high-temporal resolution approach was not confirmed to be superior to morphological assessment [3, 4]. Thus, spatial resolution has the first priority in the current standard for breast DCE-MRI, and the kinetic feature is only used with very low temporal resolution [1, 6, 7].

Although this approach of BI-RADS MRI succeeded in standardising the assessment of breast lesions and improved the diagnostic performance of DCE-MRI, the reported specificity is variable (30–97%) [8–14]. One of the reasons for this variability comes from the fact that category 4 in BI-RADS MRI has a wide range of probabilities of malignancy, extending from greater than 2% to less than 95% [1], and many benign breast lesions have to be included in category 4. At present, the additional indicators of breast MRI for discrimination between malignant and benign lesions classified as BI-RADS 4 have not been clarified.

One recently available prototype MRI sequence, time-resolved angiography with interleaved stochastic trajectories (TWIST)-volume interpolated breath-hold examination (VIBE), is known to improve the temporal resolution of DCE-MRI with preservation of spatial resolution [15–17]. This TWIST-VIBE sequence allows assessment of initial enhancement using ultra-high temporal resolution, through which both the morphological and the initial enhancement features can be evaluated in a single session.

Thus, the purpose of this study was to assess whether the measures derived from initial enhancement using TWIST-VIBE can improve the diagnostic performance of breast DCE-MRI in combination with BI-RADS, especially in BI-RADS category 4 lesions.

Materials and methods

Patients and inclusion criteria

The institutional review board approved this study, and written informed consent was obtained from each participant. The breast MRIs prospectively acquired between October 2014 and March 2016 at our institution were retrospectively evaluated. Among 317 consecutive patients who underwent 3-T breast MRI, 117 were excluded due to: history of neoadjuvant chemotherapy for breast cancers (n=44); male (n=1); contraindication to contrast agent (n=1); non-enhancing lesion on DCE-MRI (BI-RADS category 1) (n=43); and undetermined final diagnosis (n=28).

Finally, 200 patients with 215 lesions (147 malignant, 68 benign) were included in the analysis. The ages of patients with malignant lesions ranged from 35 to 84 (mean, 57) years; patients with benign lesions tended to be younger, ranging from 17 to 72 (mean, 44) years. Table 1 summarises the lesion type on MRI and the histological types of breast lesions. The diagnoses of 15 of 68 benign lesions were confirmed by clinical and imaging follow-up for at least 1.5 years after the initial MR examination.

MRI acquisition

All examinations were performed on a 3-T MR system (MAGNETOM Skyra, Siemens Healthcare GmbH, Erlangen, Germany) with a 16-channel phased-array dedicated breast coil. As in conventional DCE-MRI, a three-dimensional fat-suppressed VIBE was obtained before and two times after bolus injection of contrast agent (Fig. 1). Both breasts were

Table 1 Lesion types on MRI and histology

	Masses (n = 143)	NME (n = 59)	Focus (n = 13)
Malignant	106 (74.1)	37 (62.7)	4 (30.8)
Invasive ductal carcinoma	94	12	3
Ductal carcinoma in situ	3	22	1
Invasive lobular carcinoma	6	3	-
Mucinous carcinoma	3	-	-
Benign	37 (25.9)	22 (37.3)	9 (69.2)
Fibroadenoma	18	1	1
Benign phyllodes tumour	1	-	-
Intraductal papilloma	4	1	-
Fibrocystic change	5	15	3
Mastitis	1	3	-
Follow up (over 1.5 year)	8	2	5

NME non-mass enhancement

Unless otherwise indicated, data are numbers of lesions, with percentages in parentheses.

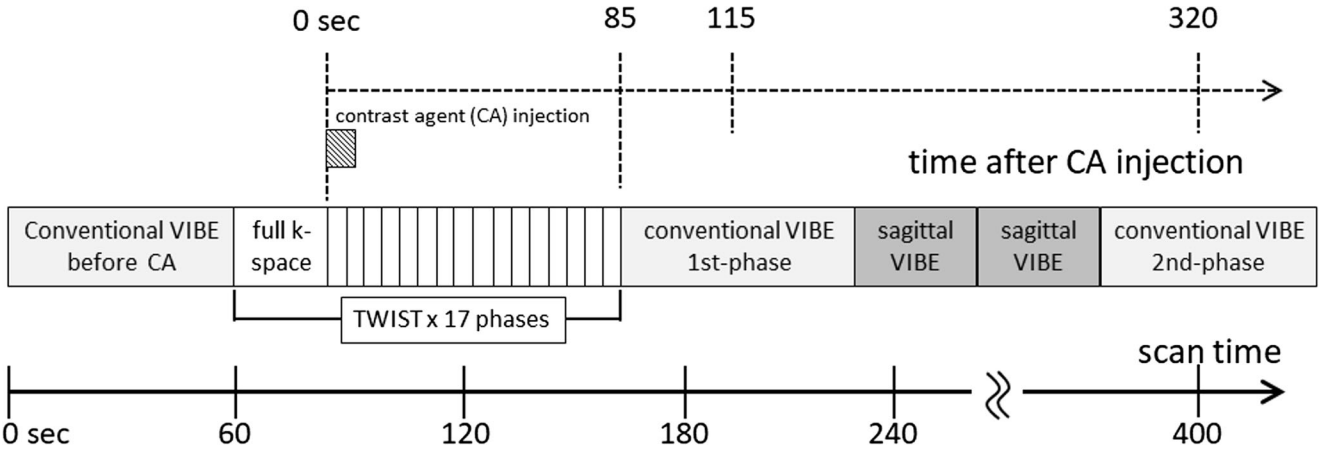

Fig. 1 Schematic timing diagrams of the dynamic contrast-enhanced protocols used in this study. The time arrow at the bottom indicates the time after the start of the scan protocol, and the upper time arrow indicates the time after the start of contrast agent injection

examined in the transverse plane. The centres of *k*-space of the first- and second-contrast phases were acquired at 115 and 320 s after contrast agent injection. Conventional VIBE parameters were as follows: repetition time ms/echo time ms, 3.3/1.4; field of view (FOV), 32 cm; matrix, 352 × 352; resolution, 1.0 × 1.0 × 1.0 mm and 144 slices; generalised autocalibrating partial parallel acquisition (GRAPPA) acceleration factor, 3; fat suppression, spectral adiabatic inversion recovery; and time of acquisition, 60 s. Between the first- and second-contrast phases of conventional VIBEs, the right and left breasts were examined sagittally using conventional VIBE with high-spatial resolution (0.7 × 0.7 × 0.8 mm), which was started from the affected side of the breasts.

The prototype TWIST-VIBE protocol was obtained between the pre-contrast and first-phase conventional VIBEs, using the transverse orientation covering both entire breasts (Fig. 1). The following imaging parameters were applied: 5.6/2.5; FOV, 36 cm; matrix, 269 × 384; resolution, 0.9 × 0.9 × 2.5 mm and 60 slices; GRAPPA, 3; fat suppression, two-point Dixon; and total scan time, 107 s (total 17 phases). The values of the TWIST view-sharing parameters *A* and *B* were selected as 15% and 10% with forward-sharing strategy, resulting in a temporal resolution of 5.3 s for each phase except the first TWIST frame (22 s, full *k*-space sampling). These values were selected based on a previous study [16]. *A* and *B* represent the percentage of the central region and of the peripheral portion of the *k*-space, respectively.

Gadoterate meglumine (Dotarem, Guerbet, Tokyo, Japan) was power-injected (Sonic Shot, Nemoto Kyorindo, Tokyo, Japan) with the beginning of the second phase of TWIST-VIBE sequences at a dose of 0.1 mmol/kg and a rate of 2 ml/s, followed by a 20-ml saline flush.

Interpretation of conventional MRI

Conventional DCE-MRI and high-spatial resolution sagittal VIBE of malignant and benign breast lesions were randomised and independently reviewed by two board-certified radiologists (M.G. and M.K., with 12 and 6 years of breast MRI experience, respectively) using the BI-RADS MR lexicon [1]. The findings on palpation, ultrasound and mammography were available for the raters for review, but they were blinded to the final pathology.

Morphological evaluation was performed using BI-RADS MRI descriptors according to the fifth edition [1]. For conventional kinetic analysis, the raters placed regions of interest (ROIs) on an interactive workstation (Aquarius, TeraRecon, Foster City, CA, USA) to evaluate the signal change of the lesion demonstrating the highest visual enhancement.

Thereafter, the raters provided a final BI-RADS assessment. The lesions that did not have any suspicious findings or findings suggestive malignancy were categorised as BI-RADS 2 (benign) or 3 (probably benign). In case of a focus, the presence of wash-out in the kinetic curve analysis was considered suspicious and would be categorised as BI-RADS 4 (suspicious). For masses and non-mass enhancement (NME), an irregular margin and rim enhancement (masses), clumped or clustered ring internal enhancement and segmental or linear distribution (NME), and wash-out kinetics (both) were considered suspicious and were classified as BI-RADS 4. In case of spiculated margin masses or irregular margin masses with rim enhancement and wash-out kinetics, and segmental or linear distribution NME with internal clumped or clustered ring enhancement, a BI-RADS 5 (highly suggestive of malignancy) was assigned [1, 14, 18, 19]. Lesions with divergent categories were then reassessed to reach a final consensual classification.

Interpretation of ultra-fast DCE-MRI

One rater (M.G.) placed ROIs using TWIST-VIBE data sets on a non-product TWIST Breast Viewer application (Siemens Healthcare GmbH) in all lesions. ROIs were placed at the descending aorta at the level of the main trunk of the

pulmonary artery to evaluate the start time of aortic enhancement and the strongest and fastest enhancing parts of the breast lesions. Two measures of initial enhancement were calculated: the time to enhancement (TTE) and the maximum slope (MS) (Fig. 2). TTE was derived from the time elapsed between the beginning of enhancement of the aorta and that of the lesion. MS was calculated from the maximal change of relative enhancement between two time points, divided by their time difference, and given as percentage relative enhancement/second [%/s].

Statistical analysis

The Mann-Whitney U test was used to compare TTE and MS values between malignant and benign groups, in all lesions, and in each lesion type on MRI, and to compare the lesion size on conventional MRI between true-positive and false-negative masses in the combined assessment. A subgroup analysis of ductal carcinoma in situ (DCIS) and invasive ductal carcinoma (IDC) was also performed using this and the Kruskal-Wallis test for each pathological prognostic factor, i.e. nuclear grade for DCIS, and histological tumour grade, hormone receptor (HR), human epidermal growth factor receptor type 2 (HER2) and Ki-67 status for IDC.

Diagnostic performance to discriminate between malignant and benign lesions was examined using receiver operating characteristic (ROC) analysis by the area under the curve (AUC) for BI-RADS, TTE and MS, and combined assessment by BI-RADS, TTE+MS using a logistic regression model. The change in AUC was tested by DeLong's test.

For the comparison of sensitivity and specificity in a clinical situation, the cases in BI-RADS 4 were reclassified using a cut-off value. The feasible cut-off values of TTE and MS were selected using the cut-off points that maximised the value of the Youden index. With the obtained cut-off value, BI-RADS 4 lesions were classified into two categories: high-suspicious (positive for malignancy) if TTE ≤ or MS ≥ cut-off value; and low-suspicious lesion (negative) if TTE > and MS < cut-off value. The combined sensitivity and specificity values were then calculated. Original BI-RADS categories of 2 or 3 were classified as benign and 4 or 5 as malignant. McNemar's test was used to compare the sensitivities and specificities of BI-RADS and BI-RADS combined with TTE+MS.

The inter-rater reliability of BI-RADS categorisation was examined by calculating the kappa coefficient. The sample size for reliability of ultra-fast DCE-MRI analysis was calculated with the following conditions: calculated sample size for the hypothesised value, 0.90; null hypothesis value, 0.60; number of ratings, two; desired α, 0.05; number of tails, two; and desired power, 0.80 [20]. Subsequently, a cohort of 14 randomly selected participants was assessed by another rater (M.K.) independently, and inter-rater reliability was examined by calculating the intraclass correlation coefficient [21].

Data were analysed using both JMP statistics software version 9.0 (version 9.0, SAS Japan) and R software (version 3.3.0, available as a free down-load from http://www.r-project.org). $p < .05$ was considered significant. The *post hoc* power analysis was performed using G*Power 3.1 (Heinrich-Heine Universitat, Dusseldorf, Germany) [22].

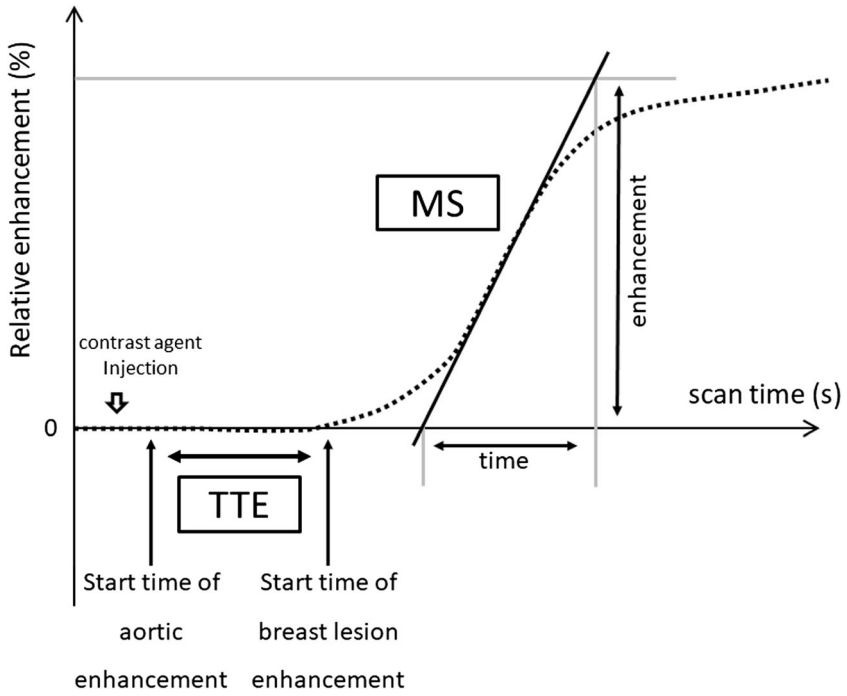

Fig. 2 Determining the time to enhancement (TTE) and maximum slope (MS) of initial enhancement using ultra-fast dynamic contrast-enhanced MRI

Results

Conventional MRI findings

Consensual BI-RADS categories and the frequencies of suspicious findings or findings highly suggestive of malignancy are summarised in Table 2. In category 4, the frequency of cancers was lower for NME and foci than for masses (53.8%, 44.4% and 82.7%, respectively). Inter-rater reliability of BI-RADS categorisation was 0.744 (95% confidence interval (CI): 0.665–0.824).

In the mass lesions, the average size on conventional MRI of malignant and benign lesions was 1.9 cm (range: 0.6–8.7 cm) and 1.6 cm (range: 0.6–6.1 cm), respectively. In the NME, the average size of malignant and benign lesions was 4.5 cm (range: 1.2–11.3 cm) and 2.5 cm (range: 0.7–5.7 cm), respectively.

Comparison of TTE and MS between malignant and benign lesions

Table 3 summarises the results. In the overall population of this study, the TTE of malignant lesions was significantly shorter than that of benign lesions (9.9 s vs. 14.0 s, p <.001), and the MS was significantly larger for malignant lesions than for benign lesions (9.8%/s vs. 5.9%/s, p <.001). The inter-rater intraclass correlation coefficient was 0.987 (95% CI: 0.960–0.996) for TTE and 0.993 (95% CI: 0.979–0.998) for MS.

For each lesion type, for masses and NME, TTE and MS showed significant differences between malignant and benign lesions. On the other hand, for foci, there were no significant differences in either TTE or MS. The powers of the Mann-Whitney tests were 0.984 and 0.523 for TTE and MS of masses, respectively, and 0.912 and 0.915 for TTE and MS of NME, respectively.

The calculated cut-off values to differentiate between malignant and benign breast lesions were 11.0 s for TTE and 7.3%/s for MS.

Diagnostic performance for masses

The results of ROC analysis for masses are summarised in Fig. 3a. The combination of BI-RADS and TTE+MS showed the highest AUC (0.864), but the difference from BI-RADS was not significant (0.823, p = .065).

The sensitivities and specificities of BI-RADS and BI-RADS combined with TTE+MS are summarised in Table 4. By the addition of TTE+MS, specificity showed a significant increase (p = .014), but the sensitivity decreased significantly (p < .001). The powers of McNemar's tests were almost 1.0 in all pairs.

Thirteen false-negative lesions were observed in the combined result; mucinous carcinoma (n=1), invasive lobular carcinoma (ILC) (n=1), DCIS (n=1) and IDC (n=10). The average size on conventional MRI of the 13 false-negative lesions (1.1 cm, range: 0.6–2.4 cm) was significantly smaller than that of 54 true-positive lesions (2.0 cm, range: 0.7–8.7 cm, p =.002). The power of the Mann-Whitney test was 0.820.

Table 2 Evaluation of cancers by BI-RADS category and findings

		Masses (n=143)			NME (n=59)			Focus (n=13)		
		No. of lesions	No. of cancers	Frequency of cancer (%)	No. of lesions	No. of cancers	Frequency of cancer (%)	No. of lesions	No. of cancers	Frequency of cancer (%)
BI-RADS category	2	4	0	0	0	0	0	0	0	0
	3	17	0	0	9	0	0	4	0	0
	4	81	67	82.7	26	14	53.8	9	4	44.4
	5	41	39	95.1	24	23	95.8	0	0	0
Suspicious findings or findings suggestive of malignancy										
Masses										
Not circumscribed margin		112	102	91.1	–	–	–	–	–	–
Rim enhancement		42	39	92.9	–	–	–	–	–	–
NME										
Segmental distribution		–	–	–	34	26	76.5	–	–	–
Linear distribution		–	–	–	0	0	0	–	–	–
Clumped		–	–	–	15	14	93.3	–	–	–
Clustered ring		–	–	–	12	12	100	–	–	–
Kinetic curve										
Wash out		95	80	84.2	33	26	78.8	9	4	44.4

BI-RADS Breast Imaging Reporting and Data System, *NME* non-mass enhancement

Table 3 Comparison of TTE and MS between and benign lesions

	TTE (sec)			MS (%/sec)		
	median	IQR	*p* values*	median	IQR	*p* values*
All lesions (n=215)						
Malignant	9.9	9.5, 13.5	<.001	9.8	7.3, 13.6	<.001
Benign	14	11.1, 17.8		5.9	3.7, 10.1	
Masses (n=143)						
Malignant	9.8	9.5, 13.3	<.001	10.6	7.5, 14.3	.006
Benign	13.5	10.7, 17.2		6.5	4.5, 12.1	
NME (n=59)						
Malignant	9.9	9.2, 12.9	<.001	9.3	7.0, 13.0	<.001
Benign	14.8	11.4, 19.0		4.5	3.5, 6.6	
Focus (n=13)						
Malignant	17.7	11.4, 22.3	.878	4.2	3.1, 5.2	.817
Benign	16.8	13.9, 20.4		4.3	3.0, 6.9	

NME non-mass enhancement, *TTE* time to enhancement, *MS* maximum slope, *IQR* interquartile range

**p* values for differences were calculated using the Mann-Whitney U test

Diagnostic performance for NME

The results of ROC analysis for NME are summarised in Fig. 3b. The AUC of combined BI-RADS and TTE+MS (0.923) was the highest, significantly different from BI-RADS alone (0.865, p =.036).

The sensitivities and specificities of BI-RADS and combined assessment are summarised in Table 4. By the addition of TTE+MS to BI-RADS, nine benign lesions categorised as BI-RADS 4 could be classified as low-suspicious lesions, and combined specificity showed a 40.9% increase (Figs. 4 and 5). There were three false-negative lesions (two DCISs and one IDC), and combined sensitivity provided an 8.1% decrease. McNemar's test showed a significant specificity increase in favour of the combined imaging (p =.005), but the difference between the sensitivities was not significant (p =.083). The powers of the McNemar tests were almost 1.0.

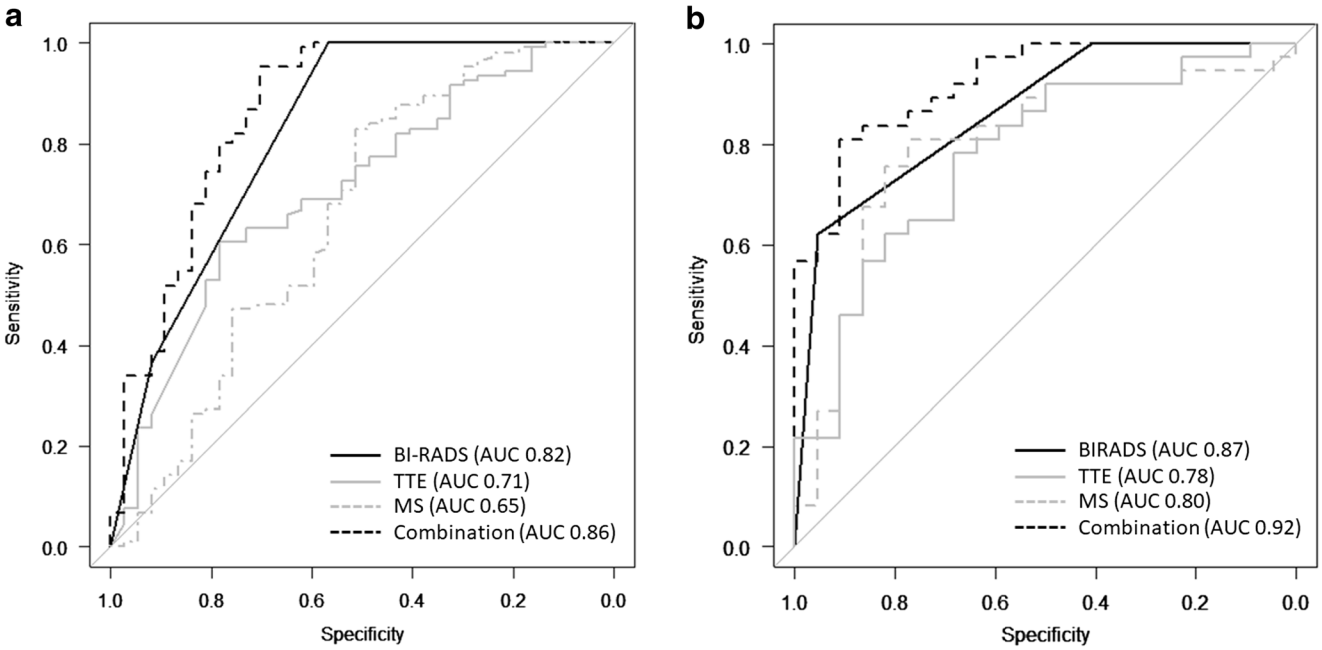

Fig. 3 Receiver operating characteristic (ROC) curves for BI-RADS, time to enhancement (TTE), maximum slope (MS) and the combination of BI-RADS and TTE+MS for masses (**a**) and non-mass enhancement (NME) (**b**). For masses, the area under the curve (AUC) is slightly improved by combining TTE+MS; however, the difference in the AUC is not significant (p = .065). For NME, the combination of BI-RADS and TTE+MS shows the highest AUC with a significant difference from BI-RADS (p = .036)

Table 4 Differentiation of category 4 lesions and diagnostic performance using TTE+MS

	No. of lesions	No. of cancer	Sensitivity (%)			Specificity (%)		
			BI-RADS	combination	*p* values*	BI-RADS	combination	*p* values*
Category 4 masses (n=81)								
Low suspicious	19	13	100	87.7	<.001	56.8	73.0	.014
High suspicious	62	54						
Category 4 NME (n=26)								
Low suspicious	12	3	100	91.9	.083	40.9	81.8	.005
High suspicious	14	11						

TTE time to enhancement, *MS* maximum slope, *BI-RADS* Breast Imaging Reporting and Data System, *NME* non-mass enhancement

**p* values for differences were calculated using McNemar's test

Correlation to histological prognostic factors

TTE and MS for each histological prognostic factor of DCIS and IDC are listed in Table 5. Biomarker status is also defined in the footnote of Table 5. The IDCs with poor histological prognostic factors (i.e. histological grade 3, HR negativity and Ki-67 positivity), except for HER2 status, had significantly shorter TTE and larger MS than the ones with good prognostic

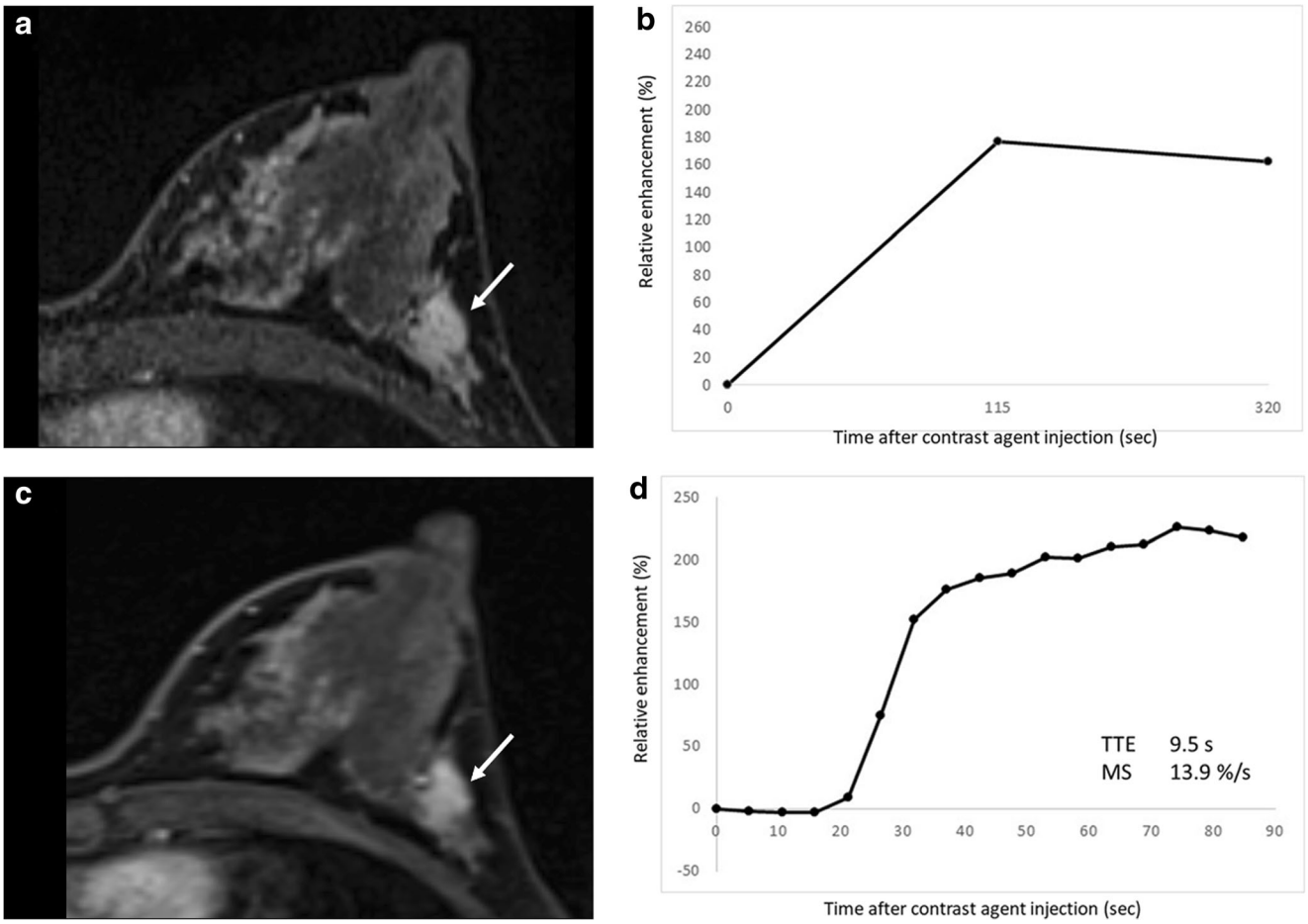

Fig. 4 Ductal carcinoma in situ in a 39-year-old woman. (**a**) Axial first-phase image of conventional dynamic contrast-enhanced MRI shows non-mass enhancement (NME) with focal distribution and heterogeneous internal enhancement (arrow). (**b**) The conventional kinetic curve of this NME is a fast-washout pattern. This NME is classified as BI-RADS category 4. (**c**) On the axial phase-17 image (about 85 s after contrast agent injection) of TWIST-VIBE, this lesion can be depicted clearly due to lower background enhancement than the conventional first-phase image (arrow). (**d**) Time-intensity curve using TWIST-VIBE shows a rapid initial rise, and the calculated TTE is 9.5 s, and MS is 13.9%/s. The combination diagnosis with BI-RADS and TTE+MS is highly suspicious for a malignant lesion

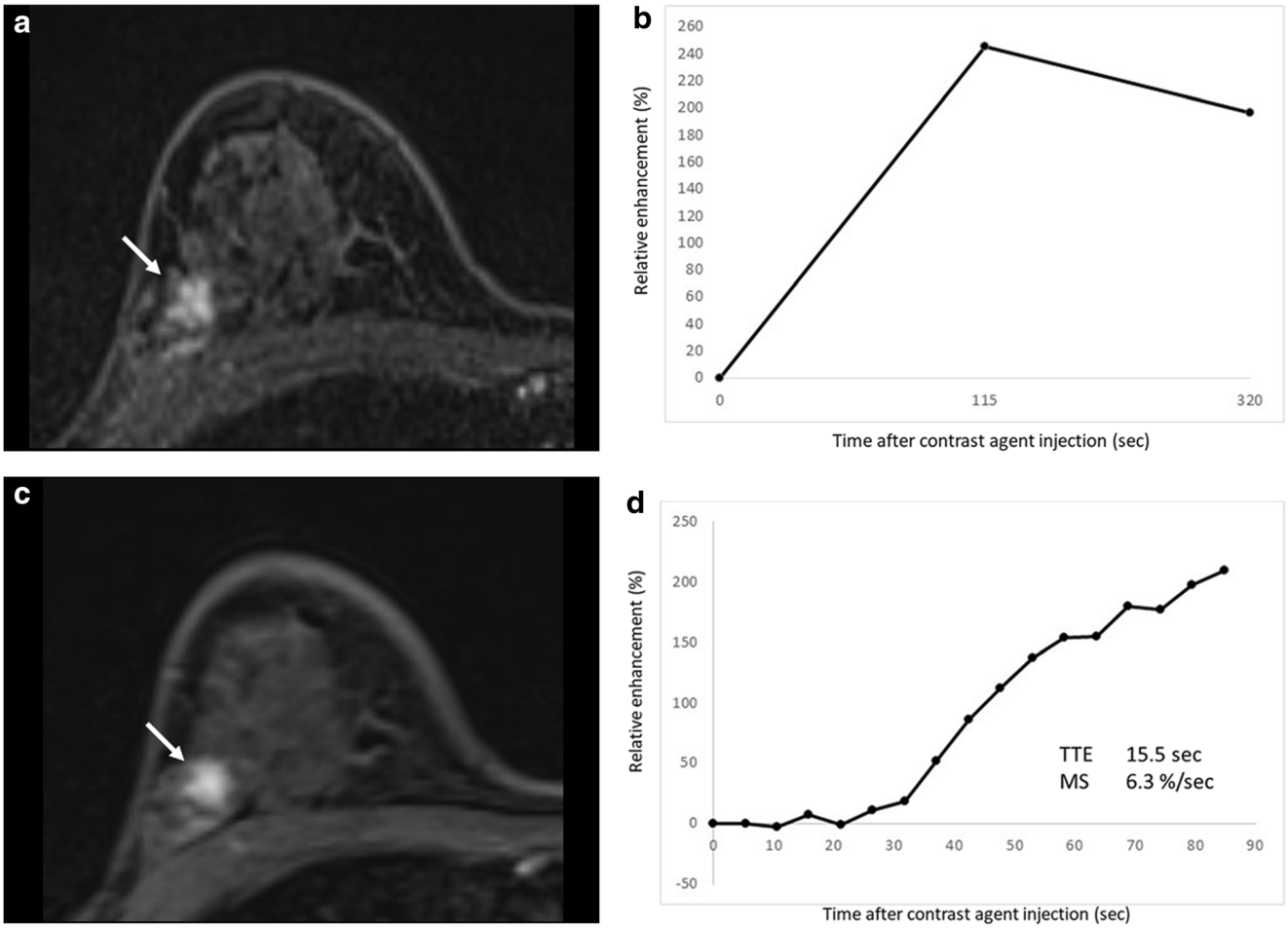

Fig. 5 Fibrocystic change in a 46-year-old woman. (**a**) Axial first-phase image of conventional dynamic contrast-enhanced MRI shows non-mass enhancement (NME) with focal distribution and heterogeneous internal enhancement (arrow). (**b**) The conventional kinetic curve of this NME is a fast-washout pattern. This NME is classified as BI-RADS category 4. (**c**) Axial phase-17 image of TWIST-VIBE; this lesion can be depicted clearly (arrow). (**d**) Time-intensity curve using TWIST-VIBE shows a persistent initial rise, and the calculated TTE and MS are 15.5 s and 6.3%/s, respectively. The combination diagnosis with BI-RADS and TTE+MS is a low-suspicious lesion

factors. In the present study, there were 11 false-negative IDCs in combined assessment and all 11 lesions (100%) were HR-positive, 10 of 11 (90.9%) were histological grade 1 or 2, and 9 of 11 (81.8%) were Ki-67-negative.

Among the DCIS cases, both TTE and MS showed no significant difference by nuclear grade.

Discussion

The present results showed that TTE and MS derived from ultra-fast DCE-MRI during initial enhancement were valuable for differentiating between malignant and benign breast lesions. By using TTE+MS effectively, category 4 NME could be divided into high- and low-suspicious lesions, and the specificity of breast MRI was shown to improve substantially.

There have been several studies that showed the utility of initial enhancement by high-temporal resolution DCE-MRI to diagnose breast lesions [2–5]. Boetes et al, using single-slice techniques, reported that contrast agent reached malignant breast lesions earlier than benign ones [4]. In the present study, TTE, which indicates the arrival time of the contrast agent from the aorta to the breast lesion, was shorter for malignant lesions than for benign lesions, which is in agreement with their results.

MS was considered a useful semi-quantitative measure, which can represent both perfusion and early leakage of contrast agent from the vessels into the extravascular extracellular space of tumours [23, 24]. MS was larger in malignant lesions than in benign ones in the present study, which is also compatible with previous results [16]. A large MS may reflect one of the characteristics of malignant lesions, in which there is histologically abundant vascularity as well as vessel wall permeability.

This is the first report to demonstrate the usefulness of initial enhancement as an addition to BI-RADS diagnosis. It is well known that BI-RADS MRI categorisation has a clinical limitation in category 4, with a wide range of probabilities of

Table 5 TTE and MS in each histologic prognostic factor

	TTE (sec)			MS (%/sec)		
	median	IQR	*p* values*	median	IQR	*p* values*
Invasive ductal carcinoma (n=109)						
Histologic grade (n=109)						
1	11.3	9.6, 15.0		9.3	6.5, 12.9	
2	9.9	9.6, 13.5	.003	9.6	7.6, 12.5	.023
3	9.4	6.9, 9.9		14.6	9.8, 18.9	
HR (n=109)[a]						
positive	10.3	9.6, 13.8	.004	9.5	7.4, 12.9	.007
negative	9.6	8.1, 9.6		14.0	9.6, 17.7	
HER2 (n=109)[b]						
positive	9.6	6.4, 11.4	.131	13.3	7.9, 17.9	.120
negative	9.9	9.6, 13.8		9.8	7.5, 13.4	
Ki-67 (n=108)[c]						
postive	9.6	8.8, 11.5	.003	11.8	8.5, 14.7	.023
negative	11.4	9.6, 14.0		9.2	6.6, 12.8	
Ductal carcinoma in situ (n=26)						
Nuclear grade						
1[d]	NA	NA		NA	NA	
2	10.9	9.5, 13.9	.428	7.5	5.0, 10.0	.330
3	9.7	7.4, 13.2		9.7	5.5, 12.8	

TTE time to enhancement, *MS* maximum slope, *IQR* interquartile range, *HR* hormone receptor, *HER2* human epidermal growth factor receptor type 2, *NA* not availavle

[a] HR positivity was define as estrogen receptor and/or progesterone receptor positivity (≥1% nuclear staining).

[b] HER2 positivity was defined as having an immunohistochemical score of 3+ or using gene amplification by means of fluorescence in situ hybridisation in tumours with an immunohistochemical HER2 score 2+.

[c] The cutoff point for Ki-67 positivity was 20%. A lesion was not available for Ki-67 status.

[d] There was no lesion classified nuclear grade 1.

**p* values for differences were calculated using the Kruskal-Wallis and Mann-Whitney U test

malignancy (2–95% [8–11]). Especially for NME, previous studies reported that the diagnostic performance of DCE-MRI was lower than for masses [6, 25–27]. The results of the present study have shown that category 4 NME had a lower cancer rate and lower specificity on BI-RADS compared with masses. By using TTE+MS, a significant specificity increase was shown by good discrimination of BI-RADS 4 NME. Therefore, the proposed initial enhancement measures may have direct impact on differentiating between malignant and benign NME, which will eliminate unnecessary biopsies.

On the other hand, both TTE and MS showed no significant differences between malignant and benign foci. For the masses, combined assessment showed a significant increase in specificity, but the sensitivity also decreased significantly. In the present study, the mean size of false-negative masses in combined assessment was smaller than that of true-positive masses. Relatively small malignant masses, including the focus, could show lower vascularity [28, 29] and poorer initial enhancement on MRI than the large lesions.

In the differentiation of BI-RADS 4 lesions using TTE+MS, DCIS and mucinous carcinoma showed higher false-negative rates than IDC in the present study. These histological types of breast cancer are well known to have lower vascular densities, and they typically show slower enhancement on DCE-MRI than IDC [30, 31]. In IDC, histological good prognostic factors may also be the reasons for underdiagnoses. Early strong enhancement was reported to correlate with high histological grade, HR negativity and Ki-67 positivity [23, 32, 33]. In fact, in the present study, the IDCs with poor histological prognostic factors had significantly shorter TTE and larger MS than the ones with good prognostic factors (Table 5).

A few recent studies have performed quantitative pharmacokinetic analysis using ultra-fast sequences [22, 23, 34, 35]. These model-based approaches make it possible to calculate absolute values that are directly related to tissue perfusion, capillary permeability and other physiological and anatomical features. However, they involve complicated image post processing that requires adequate arterial input function and T1 mapping. The semi-quantitative measures used in our study

are much simpler and showed high inter-rater reliability. We believe that this semi-quantitative analysis is sufficient for clinical usage.

One of the attempted ways to increase the specificity of breast MRI without contrast medium is to evaluate apparent diffusion coefficient (ADC) values obtained from diffusion-weighted imaging (DWI) [13, 14, 25, 26]. However, there have been only a few reports regarding the utility of DWI in NME [25, 26]. This probably is due to the fact that NME is difficult to visualise on the ADC map, and the reliability of ADC value measurement is lower than for mass lesions. Compared with DWI, TWIST-VIBE has much higher spatial resolution, and it clearly visualises the enhancing lesions, making it much easier to place the ROIs.

T2-weighted imaging (T2WI) may also be helpful to differentiate malignant and benign NMEs. Past studies reported that microcysts on T2WI may be among the findings of benign fibrocystic change [36], and others reported that surrounding oedema of NME was a predictor of malignancy, especially in invasive cancer [37, 38]. However, the reported frequencies of these findings for each benign and malignant NME were insufficient, and it is still unclear whether T2WI contributes to increasing the specificity of breast MRI.

This study had several limitations. First, the early post-contrast phase of conventional VIBE was slightly later in timing after contrast agent injection, and this fact may have influenced the conventional kinetic and morphological assessment. However, the centre of *k*-space of this first-phase (115 s) was in line with BI-RADS determination (i.e. <120 s), and spatial resolution was preserved. In addition, the high-spatial resolution sagittal VIBE was evaluated together. We believe that preserved high-spatial resolution made it possible for clinically feasible and good inter-rater reliabilities of the lesion morphology in the present study [6, 7]. The prevalence of malignant lesions that showed delayed wash-out kinetics in the present study was also consistent with previous reports (Table 2) [26, 27]. Second, a large portion of the lesions was malignant, and there were many invasive cancers and few benign lesions. This is caused by our study population including only cases that had a clinical indication for breast MRI. Third, the proposed cut-off values for MS and TTE may depend on many technical parameters such as contrast dose and specific scan protocol settings, and these need to be verified in future studies.

In summary, we have presented an approach to initial enhancement analysis derived from TWIST-VIBE. The measures TTE and MS not only showed good separation between malignant and benign breast lesions, but they also provided added diagnostic value to BI-RADS category 4 NME. We believe that this is a feasible way to increase the specificity of breast MRI, and it is conceivably an important step towards decreasing the number of unnecessary biopsies.

Funding This study has received funding by the Japan Society for the Promotion of Science (JSPS) KAKENHI Grant Number JP16K19840.

Compliance with ethical standards

Guarantor The scientific guarantor of this publication is Mariko Goto MD, PhD, Assistant Professor of the Department of Radiology, Kyoto Prefectural University of Medicine.

Conflict of interest The authors of this manuscript declare relationships with the following companies: Two of the co-authors (Elisabeth Weiland and Hiroshi Imai) are employees of Siemens Healthcare.

Statistics and biometry One of the authors (Isao Yokota) has significant statistical expertise.

Informed consent Written informed consent was obtained from all subjects (patients) in this study.

Ethical approval Institutional Review Board approval was obtained.

Methodology
- Retrospective
- Diagnostic or prognostic study
- Performed at one institution

References

1. American College of Radiology Breast Imaging Reporting and Data System (BI-RADS), vol 2013, 5th edn. American College of Radiology, Reston, VA
2. Helbich TH, Roberts TP, Gossmann A et al (2000) Quantitative gadopentetate-enhanced MRI of breast tumors: testing of different analytic methods. Magn Reson Med 44:915–924
3. Gibbs P, Liney GP, Lowry M, Kneeshaw PJ, Turnbull LW (2004) Differentiation of benign and malignant sub-1 cm breast lesions using dynamic contrast enhanced MRI. Breast 13:115–121
4. Boetes C, Barentsz JO, Mus RD et al (1994) MR characterization of suspicious breast lesions with a gadolinium-enhanced TurboFLASH subtraction technique. Radiology 193:777–781
5. Sardanelli F, Rescinito G, Giordano GD, Calabrese M, Parodi RC (2000) MR dynamic enhancement of breast lesions: high temporal resolution during the first-minute versus eight-minute study. J Comput Assist Tomogr 24:724–731
6. Goto M, Ito H, Akazawa K et al (2007) Diagnosis of breast tumors by contrast-enhanced MR imaging: comparison between the diagnostic performance of dynamic enhancement patterns and morphologic features. J Magn Reson Imaging 25:104–112
7. Kuhl CK, Schild HH, Morakkabati N (2005) Dynamic bilateral contrast-enhanced MR imaging of the breast: trade-off between spatial and temporal resolution. Radiology 236:789–800
8. Rosen EL, Baker JA, Soo MS (2002) Malignant lesions initially subjected to short-term mammographic follow-up. Radiology 223:221–228
9. Ikeda DM, Baker DR, Daniel BL (2000) Magnetic resonance imaging of breast cancer: clinical indications and breast MRI reporting system. J Magn Reson Imaging 12:975–983
10. Malich A, Boehm T, Facius M et al (2001) Differentiation of mammographically suspicious lesions: evaluation of breast ultrasound, MRI mammography and electrical impedance scanning as

adjunctive technologies in breast cancer detection. Clin Radiol 56: 278–283
11. Malich A, Fischer DR, Wurdinger S et al (2005) Potential MRI interpretation model: differentiation of benign from malignant breast masses. AJR Am J Roentgenol 185:964–970
12. Peters NH, Borel Rinkes IH, Zuithoff NP, Mali WP, Moons KG, Peeters PH (2008) Meta-analysis of MR imaging in the diagnosis of breast lesions. Radiology 246:116–124
13. Dijkstra H, Dorrius MD, Wielema M, Pijnappel RM, Oudkerk M, Sijens PE (2016) Quantitative DWI implemented after DCE-MRI yields increased specificity for BI-RADS 3 and 4 breast lesions. J Magn Reson Imaging 44:1642–1649
14. Kul S, Cansu A, Alhan E, Dinc H, Gunes G, Reis A (2011) Contribution of diffusion-weighted imaging to dynamic contrast-enhanced MRI in the characterization of breast tumors. AJR Am J Roentgenol 196:210–217
15. Le Y, Kipfer H, Majidi S et al (2013) Application of Time-Resolved Angiography With Stochastic Trajectories (TWIST) -Dixon in Dynamic Contrast-Enhanced (DCE) Breast MRI. J Magn Reson Imaging 38:1033–1042
16. Mann RM, Mus RD, van Zelst J, Geppert C, Karssemeijer N, Platel B (2014) A novel approach to contrast-enhanced breast magnetic resonance imaging for screening: high-resolution ultrafast dynamic imaging. Invest Radiol 49:579–585
17. Mus RD, Borelli C, Bult P et al (2017) Time to enhancement derived from ultrafast breast MRI as a novel parameter to discriminate benign from malignant breast lesions. Eur J Radiol 89:90–96
18. Tozaki M, Fukuma E (2009) 1H MR spectroscopy and diffusion-weighted imaging of the breast: are they useful tools for characterizing breast lesions before biopsy? AJR Am J Roentgenol 193:840–849
19. Maltez de Almeida JR, Gomes AB, Barros TP, Fahel PE, de Seixas Rocha M (2015) Subcategorization of Suspicious Breast Lesions (BI-RADS Category 4) According to MRI Criteria: Role of Dynamic Contrast-Enhanced and Diffusion-Weighted Imaging. AJR Am J Roentgenol 205:222–231
20. Zou GY (2012) Sample size formulas for estimating intraclass correlation coefficients with precision and assurance. Stat Med 31: 3972–3981
21. Matsuoka T, Imai A, Fujimoto H et al (2017) Reduced Pineal Volume in Alzheimer Disease: A Retrospective Cross-sectional MR Imaging Study. Radiology 286:239–248
22. Faul F, Erdfelder E, Lang AG, Buchner A (2007) G*Power 3: a flexible statistical power analysis program for the social, behavioral, and biomedical sciences. Behav Res Methods 39:175–191
23. Koo HR, Cho N, Song IC et al (2012) Correlation of perfusion parameters on dynamic contrast-enhanced MRI with prognostic factors and subtypes of breast cancers. J Magn Rson Imaging 36: 145–151
24. Li SP, Padharni AR, Taylor NM et al (2011) Vascular characterization of triple negative breast carcinomas using dynamic MRI. Eur Radiol 21:1364–1373
25. Imamura T, Isomoto I, Sueyoshi E et al (2010) Diagnostic performance of ADC for Non-mass-like breast lesions on MR imaging. Magn Reson Med Sci 9:217–225
26. Yabuuchi H, Matsuo Y, Kamitani T et al (2010) Non-mass-like enhancement on contrast-enhanced breast MR imaging: lesion characterization using combination of dynamic contrast-enhanced and diffusion-weighted MR images. Eur J Radiol 75:126–132
27. Tozaki M, Igarashi T, Fukuda K (2006) Positive and negative predictive values of BI-RADS-MRI descriptors for focal breast masses. Magn Reson Med Sci 5:7–15
28. Schnall MD, Blume J, Bluemke DA et al (2006) Diagnostic architectural and dynamic features at breast MR imaging: multicenter study. Radiology 238:42–53
29. Kim SH, Lee HS, Kang BJ et al (2016) Dynamic Contrast-Enhanced MRI Perfusion Parameters as Imaging Biomarkers of Angiogenesis. PLoS One. https://doi.org/10.1371/journal.pone.0168632
30. Monzawa S, Yokokawa M, Sakuma T et al (2009) Mucinous carcinoma of the breast: MRI features of pure and mixed forms with histopathologic correlation. AJR Am J Roentgenol 192:125–131
31. Orel SG, Mednonca MH, Reynolds C, Schnall MD, Solin LJ, Sullivan DC (1997) MR imaging of ductal carcinoma in situ. Radiology 202:413–420
32. Szabó BK, Aspelin P, Kristoffersen Wiberg M, Tot T, Boné B (2003) Invasive breast cancer: correlation of dynamic MR features with prognostic factors. Eur Radiol 13:2425–2435
33. Baltzer PA, Vag T, Dietzel M et al (2010) Computer-aided interpretation of dynamic magnetic resonance imaging reflects histopathology of invasive breast cancer. Eur Radiol 20:1563–1571
34. El Khouli RH, Macura KJ, Kamel IR, Jacobs MA, Bluemke DA (2011) 3-T dynamic contrast-enhanced MRI of the breast: pharmacokinetic parameters versus conventional kinetic curve analysis. AJR Am J Roentgenol 197:1498–1505
35. Yi B, Kang DK, Yoon D et al (2014) Is there any correlation between model-based perfusion parameters and model-free parameters of time-signal intensity curve on dynamic contrast enhanced MRI in breast cancer patients? Eur Radiol 24:1089–1096
36. Milosevic ZC, Nadrljanski MM, Milovanovic ZM, Gusic NZ, Vucicevic SS, Radulovic OS (2017) Breast Dynamic Contrast Enhanced MRI: Fibrocystic Changes Presenting as a Non-mass Enhancement Mimicking Malignancy. Radiol Oncol 51:130–136
37. Yuen S, Uematsu T, Masako K, Uchida Y, Nishimura T (2008) Segmental enhancement on breast MR images: differential diagnosis and diagnostic strategy. Eur Radiol 18:2067–2075
38. Uematsu T, Kasami M (2012) High-spatial-resolution 3-T breast MRI of nonmasslike enhancement lesions: an analysis of their features as significant predictors of malignancy. AJR Am J Roentgenol 198:1223–1230